High resolution numerical simulation of precipitating events: On the importance of initial humidity field

V. Ducrocq, M. Nuret, J.P. Lafore and D. Ricard

CNRM/GMME (Météo-France & CNRS)
Toulouse, France

1. Introduction

A number of national meteorological centres plans to run operationally before the end of the decade numerical weather prediction systems with horizontal resolution of only several kilometres. These models would be non-hydrostatic with advanced parameterisation of physical processes (complex microphysics, 3D turbulence,…). In most cases, sub-grid convection scheme would not be required, as the horizontal resolution allows to explicitly resolved the convection at that scale. So that, given the same initial conditions, the forecast of these models could be very different to those of the actual operational models (Ducrocq et al, 2002). It is therefore essential to study the impact of assimilation techniques or of new observations on the forecasts of such high numerical models.

The initial humidity field is a key parameter for the simulation of convection, so that we have focused our efforts at CNRM/GMME on observations that can supply directly or indirectly some information about the mesoscale structure of the humidity field: mesoscale surface observations, satellite data and radar reflectivities. In order to extract a humidity information from the two latter types of data, we have developed pre-processings of cloud and precipitation areas. In the first study presented in section 4, the prep-processing of cloud and precipitation areas is based mainly on radar reflectivities, while in the second study presented in section 5, it is based mainly on a cloud classification.

2. The MESO-NH model

The MESO-NH model (Lafore et al, 1998) is a non-hydrostatic numerical model developed by Météo-France and the Laboratoire d'Aérologie for research purposes. It is able to simulate atmospheric motions ranging from the synoptic scale to turbulent large eddies. Among the three anelastic systems that are coded in MESO-NH, we use here the pseudo-incompressible system of Durran (1989). The two way interactive grid nesting technique of Clark and Farley (1984) has been implemented in MESO-NH : the coarser grid provides the lateral boundary condition to the finer grid, while the variables of the coarser grid are relaxed with a short relaxation time towards the model trajectory of the finer grid on the overlapping area.

The equations of the model are written on a conformal plan and the vertical coordinate is the Gal-Chen and Sommerville (1975)'s coordinate. The prognostic variables are the three-dimensional wind components, the potential temperature, the mixing ratios of the different water phases and the turbulent kinetic energy. A bulk microphysical scheme (Caniaux et al , 1994) governs the equation of the six water species (vapour, cloud water, liquid water, primary ice, snow and graupel). Except for the horizontal resolutions finer than about 5 km, the sub-grid scale convection is parameterised by the Kain and Fritsch (1993) scheme, adapted to MESO-NH by Bechtold et al (2001). Also, the turbulence scheme is three-dimensional for the finer grids, while the horizontal gradients are not considered for coarser resolution.

It is important to note that MESO-NH has no analysis component. So that the standard version of MESO-NH starts from interpolation of large scale operational analyses such as the ECMWF or ARPEGE analyses.

3. The mesoscale observations

The mesoscale observations used in our studies are the following :

Radar data : The operational radar network of METEO-FRANCE, called ARAMIS, provides PPI reflectivities with 1km^2 pixels at temporal frequency of 5 minutes. Mosaic imagery gathers individual radar data on a 1.5 km resolution grid.

Satellite data : We focus on METEOSAT data due to their high temporal frequency (temporal and spatial resolutions of 30 minutes and 6 kilometers). Moreover, METEO-FRANCE produces operationally a cloud classification over western Europe based on IR and VIS imagery from METEOSAT at 1 hour frequency and 6 kilometers resolution. This cloud classification is based on the dynamic clustering method of Desbois et al (1982) and distributes the pixels in sixteen cloud classes (Table 1).

Surface observations : The French surface observations network is well provided since the automatic ground stations are spaced in average by 30 kilometers. There are more than a thousand observations of 2-meter temperature and due point temperature and about 800 observations of 10- meter winds. They are available in the central archive at one hour resolution.

Cloud class	Cloud Type	Associated Cloud layer		
		High	Medium	Low
1	clear			
2	cloud edge 1	undefined	undefined	undefined
3	cloud edge 2	undefined	undefined	undefined
4	thin cirrus	X	undefined	undefined
5	thick cirrus	X	undefined	undefined
6	cirrostratus	X	undefined	undefined
7	nimbostratus (perturbation body)	X	X	X
8	Small cumulus			X
9	cumulus of moderate extent		X	X
10	cumulonimbus calvus		X	X
11	stratus/fog			X
12	stratocumulus			X
13	altocumulus/altostratus1		X	undefined
14	altocumulus/altostratus 2		X	undefined
15	altocumulus/altostratus 3		X	undefined
16	very thick cloud, cumulonimbus	X	X	X

Table 1 : *The cloud classification and the associated cloud layers*

4. Meso-g scale adjustment and assimilation based on radar data

4.1. Description of the method

In this part, we describe briefly the static fine scale initialisation procedure of Ducrocq et al (2000) that uses mesoscale surface observations and radar data to provide a better description of the meso-β scale low-level environment in which the convective systems form together with a meso-γ scale description of the convective systems. Recently, this procedure has been extended to offer the possibility of performing a Newtonian relaxation during the first time of the simulation.

STEP1 : Mesoscale surface observations analysis

The first step of the fine scale initialisation procedure of Ducrocq et al (2000) updates the background fields with mesonet surface observations. The IO scheme, called DIAGPACK and linked to the ALADIN limited area model, is used for that purpose. Upper analyses of wind, temperature and relative humidity are performed with surface observations as input data to modify the low levels of the atmosphere. Besides, analyses of 2 meters temperature, 2 meters relative humidity, 10 meters wind and surface pressure work separately; the increments from these analyses are used to modify the soil variables. According to the network density, the analysis scheme has been tuned in order to better describe the meso- βscale structures (Calas et al, 2000). The background can be provided either by a short-range forecast of ALADIN or by ARPEGE or ECMWF analyses interpolated on a 10-km domain. This analysis provides the initial state of all nested domains.

STEP2a : Precipitation and cloud pre-processing

A cloud and precipitation analysis is performed for the finer domain. It begins by interpolating both the input data and background fields provided by STEP 1 on the model grid. Then, model column is assumed to be rainy and cloudy if the radar reflectivity at this grid point is above 12 dBz. Moreover, a model column can also be cloudy if the infrared brightness temperature is colder than the background surface temperature by a fixed temperature threshold (8 K) and if the column is located within about 10 km from the rainy area. Then for each cloudy column, the cloud top height is derived by facing the IR brightness temperature with the background temperature profile. The cloud base height is given by the lifting condensation level of the surface parcel of the background fields.

STEP2b: Humidity and microphysical adjustment based on the precipitation and cloud preprocessing

Then, the cloud and precipitation analysis drives a moisture and microphysical adjustment that is superimposed on the initial state of the finer grid. This adjustment is such that the vapour mixing ratio inside the cloudy areas is set to its saturated value. For each rainy column, rainwater is imposed below the freezing level, and snow replaces rainwater above it. As only single PPI is available, an empirical vertical profile of snow and rainwater has to be inferred from the reflectivity value on the PPI.

STEP3: Newtonian relaxation based on the precipitation and cloud pre-processing

In that case, STEP 2a is performed at each time step of the finest domain during the first time of the simulation, using as input linear temporal interpolations of reflectivity data and satellite data. Then, the model vapor mixing ratio is nudge toward its saturated value inside cloudy areas that are detected at each time step.

4.2. Experimental design

The fine scale static initialisation has been tested on four convective cases : 4 Aug. 1994 (hereafter case A), 13 May 1998 (case B), 3-4 Oct 1995 (case C), 13-14 Oct. 1995 (case D). Cases A and B are over flat areas in

northern France, while the two others are over more mountainous areas in south-eastern France. These cases formed with weak synoptic forcing.

Table 2 presents the numerical experiments performed on these convective cases. All the simulations used two nested domains at 10 km and 2.5 km horizontal resolution. The CTRL experiments start from the ARPEGE (or ECMWF) analysis. For the INIT experiments, steps 1 to 2 have been applied to produce their initial conditions. They are applied one hour after the observed triggering of the convection. The background is supplied by a short range forecast of ALADIN. The SURF experiments have as initial conditions only the mesoscale surface observations analysis (STEP 1). For the NUDG experiment which has the same initial conditions as the INIT experiment, the model vapour mixing ratio is nudged (STEP 3) during a pre-forecast period of one hour with a relaxation coefficient of 8 10^{-4} s^{-1}.

Experiments	**Initial Conditions**	**Studied Convective Cases**
CTRL	ECMWF or ARPEGE analysis	Cases A, B, C and D
INIT	Mesoscale surface observation analysis + Humidity and microphysical adjustment based on radar and IR data	Cases A, B, C and D
SURF	Only the mesoscale surface observation analysis	Cases A, B, C and D
NUDG	Same as INIT + Newtonian relaxation based on radar and IR data	Cases A and D

Table 2 : *Description of the numerical experiments performed on the several convective cases over France.*

4.2.1. Results

Figure 1 presents the reflectivities diagnosed from the simulated hydrometeor mixing ratio for the experiments CTRL and INT for the four cases. It can be seen that the INIT experiments improve results in all cases. For example, for case A, the CTRL experiment does not produce any echo while the INIT experiment produces a convective line as observed. For case D, the CTRL experiment produces an area of echoes which are not organized in a line and with a limited vertical extension (below 5km), while the INIT experiment represents a quasi-stationary convective line that is well developed (up to the tropopause). For the two other cases (B and C), only small areas of echoes are shown in CTRL experiments, while the INIT experiments produces reflectivity organisations that look like the observed reflectivity. This better behaviour of the INIT experiments have been also confirmed with objective scores between the rain gauges and the simulations on accumulated surface precipitation over the complete duration of the INIT simulation. Figure 2 shows these objective scores that have been computed on 2x2 contingency tables for cases A, C and D for the CTRL, INIT and SURF experiments. (Scores cannot be computed for the case B, as the density of the rain gauge network does not allow the precipitation event to be captured). The thresholds vary from one case to the others and correspond to the highest threshold with at least 10 to 15 percent of observations above the threshold value. For cases A and C, the CTRL experiments don't forecast values above the threshold, so that the scores on the contingency tables are zero or undefined. For case D, the scores show also an improvement of the surface rainfall forecast compared with the CTRL experiment.

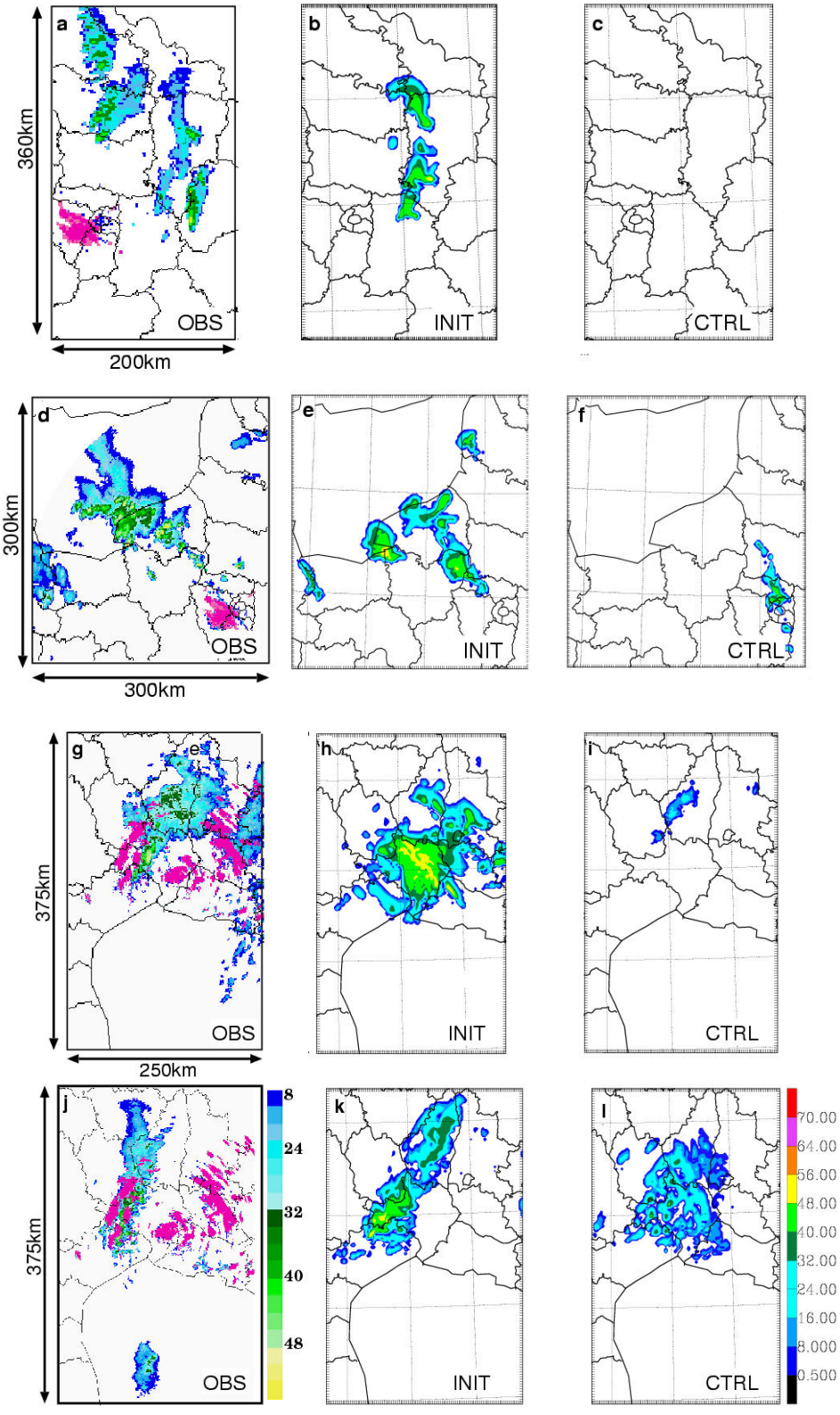

Figure 1 : *Reflectivities from the observations (left column), from the INIT experiments (middle column) and from the CTRL experiments (right column) for : (a,b,c) Case A at 18 UTC, 4 Aug. 1994; (d,e,f) Case B at 17 UTC, 13 May 1998; (g,h,i) Case C at 04 UTC, 4 October 1995; (j,k,l) Case D at 03 UTC, 14 October 1995. The observed reflectivities are PPI radar reflectivities (ground echoes are in pink). Reflectivities of the experiments are diagnosed from the simulated hydrometeor fields around 2km.*

The SURF experiments allow to evaluate the specific impact of the mesoscale surface data analysis in the initialisation procedure of Ducrocq et al (2000). For the two cases of convection over the French northern plains, the two parts of the initialisation method are required; the mesoscale surface data analysis alone does not allow a good representation of the convective system, as can be seen with the objective scores on case A (Fig. 2) or with the fields of 3-hour accumulated surface rainfall (Fig. 3). For the two other cases of convection that occurred over mountainous areas, the differences between the INIT and SURF experiments are not so important. The scores are quite similar between the two types of experiments for cases C and D. This different sensitivity to the initial conditions from cases C and D to cases A and B can be explained by the environmental conditions and the type of convection. For cases A and B, the convective systems appeared in quite dry atmospheres over flat areas and are driven by a cold pool linked to the evaporation of falling precipitation. So that, the moisture and microphysical adjustments allow the release of the convective instability by moistening the convective system area and the surface data analysis helps to organize the convection by introducing a cold pool beneath the storm. On the contrary, the convective systems of cases C and D develop in a moist environment and are fed by converging nearly saturated low-level flows running over the Massif Central Foothills. The mesoscale surface data analysis improves the description of this low-level moist flow, while the moisture and microphysical adjustments do not increase significantly the humidity as the middle and upper layers were already moist. The topography and the induced circulations play a major role for this second type of systems.

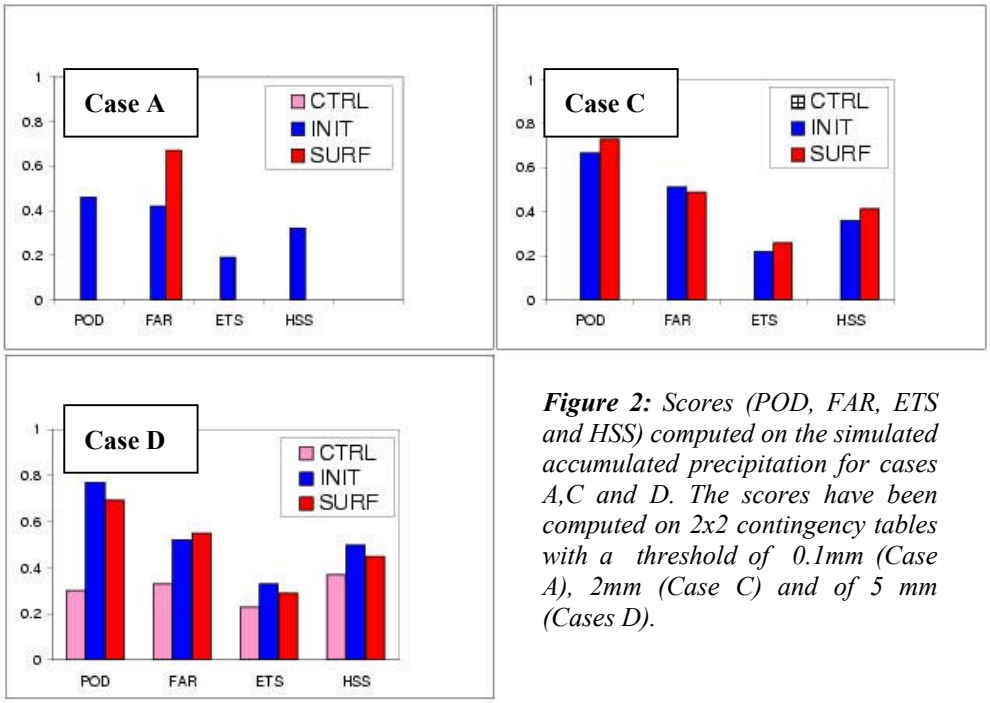

Figure 2: *Scores (POD, FAR, ETS and HSS) computed on the simulated accumulated precipitation for cases A,C and D. The scores have been computed on 2x2 contingency tables with a threshold of 0.1mm (Case A), 2mm (Case C) and of 5 mm (Cases D).*

When Newtonian relaxation is added (NUDG experiments), the results are slightly improved (Fig. 4). For the reasons given below, the impact is larger for the convective case over the northern plains than for the convective case over the Massif Central.

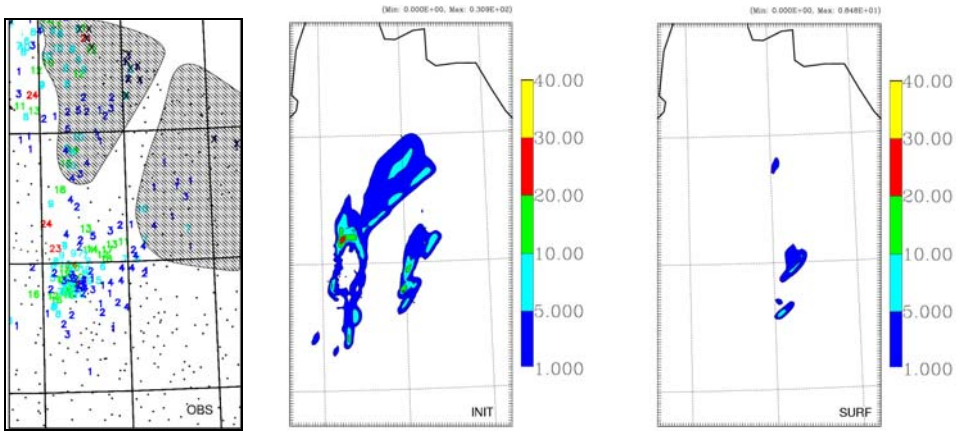

Figure 3: *The accumulated surface rainfall for Case A : a) from 06 UTC 4 August 1994 to 06 UTC 5 August 1994 for the observations; b) from 15 UTC to 18UTC for the INIT experiment; c) from 15 UTC to 18UTC for the SURF experiment. The observed values have been crossed when the totality of the precipitation at this point was linked to radar echoes occurring all after 18 UT, while the hatched areas, a part of the precipitation occurred after 18 UTC.*

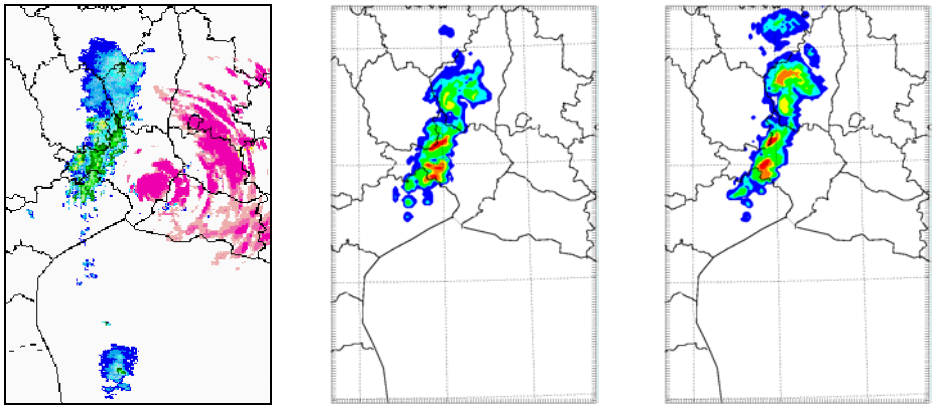

Figure 4 *: Reflectivities for Case D (at 2 UTC 14 October 1995) : a) from the observation; b) from the INIT experiment; c) from the NUDG experiment. Same color scale as in Fig. 1*

5. Meso-β scale analyses based on a satellite-based cloud classification

5.1. Description of the method

In this part, we describe the method that has been developed to use a cloud classification in order to derive humidity information that are afterwards analysed with an OI scheme.

STEP A: Cloud pre-processing

First, a nebulosity for the high, medium and low cloud layers is associated to each pixel of the cloud-classification (Table 1). For example, for a pixel in the cumulus class, the nebulosity is zero for the high and medium cloud layers and of 1 for the low cloud layer. Note that the nebulosity of cloud layers may be undefined in case of high or medium clouds or in case of cloud edges. Then a cloud fraction is computed on the regular grid associated with the model. The cloud fraction for the three cloud layers is evaluated by counting the number of cloudy pixels of the satellite-based cloud classification inside the model grid box. The averaged IR cloud top temperature is computed for each layers. It is then used for the cloud top height assignment by facing this IR temperature with the model background temperature profile. For those clouds

whose expected cloud base belong to the low layer, the cloud base height is given by the lifting condensation level of the surface parcel of the model background profile. For the other clouds, a prescribed thickness is assumed (2000 m for high clouds and 1500 m for medium clouds).

STEP B : Radar constraints

In some experiments, the ARAMIS composite reflectivities have been used to correct the cloud classification which sometimes shows difficulties in correctly assign Cirrus type and Cumulonimbus type. For pixels assigned to the Cirrus classes (classes 4, 5 and 6), they are converted into thick and deep cloud (class 16) if radar reflectivitiy is above 8 dBz and vice-versa. In that case, the use of the cloud classification is restrained to the area covered by the ARAMIS radars.

STEP C : Analysis of derived-cloud data

A relative humidity profile is determined at each model column for cloud fraction equal to 1 (completely covered) or to zero (clear profile). The prescribed values of relative humidity have been calibrated with radio-soundings taken inside the cloudy perturbation body and inside the clear sky area for the studied day and its surroundings. So that, the relative humidity is imposed to 20% for the clear profiles, while for cloudy profiles, the relative humidity increases from 90 % at 800 hPa to 95 % at about 700hPa and decreases above 700hPa to reach 85 % at about 500 hPa. The humidity profile is never produced at low levels (150 hPa above the surface).

Then, these humidity profiles are analysed with the OI DIAGPACK scheme which has been tuned to represent meso-βscales. For example, the characteristic length scale for the humidity model error has been set to 60 km at surface level and 200 km at 500 hPa.

5.2. Experimental design

The impact of using cloud classification data has been evaluated on the IOP14 of MAP (Bougeault et al, 2001) which corresponds to a strong convective event over the Laggo Maggiore area. This convection was associated with a slow moving upper level trough which evolved in a cut-off low over the Mediterranean sea. Table 3 describes the different numerical experiments. Experiments suffixed by 1 used two nested domains at 30 km and 10 km horizontal resolutions, while experiments suffixed by 2 used three nested domains at 30, 10 and 2.5 km resolutions. So, that the impact both at parameterised convection scale and at resolved convection scale can be evaluated.

All the experiments start at 12 UTC, the 2nd November 1999. The CTRL experiments start from the 12 UTC ECMWF analysis. For the SAT experiments, the initial state is produced by the analysis of humidity profiles deduced of the cloud classification (STEPs A+C), the background being the 12 UTC ECMWF analysis. The SAT_RAD experiments are the same as the SAT experiments except that the radar constraints apply (STEPs A+B+C). For the SAT_RAD_SURF experiments, mesoscale surface observations are also analysed as in part 4 (STEPs A+B+C and STEP 1). The SURF experiments have only the mesoscale surface observation analysis as initial conditions (STEP 1).

Experiments	**Number and Resolution of the models**	**Initial conditions**
CTRL1	2 30 km and 10 km	12 UTC, 2 Nov. 1999 ECMWF analysis
SAT1	Idem CTRL10	Analysis of synthetic humidity profiles based on cloud classification
SAT_RAD1	Idem CTRL10	Same as SAT1 + Radar reflectivity constraints
SAT_RAD_SURF1	Idem CTRL10	Same as SAT_RAD1 + mesoscale surface observation analysis
SURF1	Idem CTRL10	Only the mesoscale surface observation analysis
CTRL2	3 30 km, 10 km and 2.5 km	12 UTC, 2 Nov. 1999 ECMWF analysis
SAT2	Idem CTRL2	Analysis of synthetic humidity profiles based on cloud classification
SAT_RAD_SURF 2	Idem CTRL2	Same as SAT2 + Radar reflectivity constraints + mesoscale surface observation analysis
SURF2	Idem CTRL2	Only the mesoscale surface observation analysis

Table 3 : *Description of the numerical experiments performed on the IOP14 of MAP*

5.3. Results

Figure 5 presents the 6-hour cumulated surface rainfall between 12UTC and 18UTC for the observations and for the 10 km domain of the CTRL1, SAT1, SAT_RAD1, SAT_RAD_SURF1 and SURF1 experiments. The line AB indicates the axis of main core of observed precipitation associated to the front crossing France. In the CTRL1 experiment, the front is shifted of about 100 km compared to the line AB. The two experiments that position best the front are the SURF1 and SAT_RAD_SURF1 experiments, while the SAT1 experiment supplies a better representation of the post-frontal activity.

Objectives scores on 6-hour cumulated rainfall have been computed for the first 24 hours of the simulations (Fig. 6a). All the experiments with modified initial conditions give better scores than the CTRL1 experiments. The SAT1 experiment gives better score for the weak thresholds (0.1mm, 1 mm), while it is the SAT_RAD_SURF1 experiment that shows better scores for the 5 mm and 10 mm thresholds. Combining the mesoscale surface observation analysis with the analysis of synthetic humidity profiles improves the results. A positive impact of the modified initial conditions is found globally until 24-hour range, but the largest positive impact is found for the 06-12UTC range forecast(Fig. 6b).

As can be seen on Figure 7, the impact of the modified initial conditions is globally the same for the 2.5 km domain : the SAT_RAD_SURF2 and SURF2 experiments improve the location of the front. The ETS scores on the cumulated surface rainfall tends to show a slight improvement when the resolution is increased (Fig. 8). The SAT_RAD_SURF2 experiment (Fig. 7c) tends to overestimate the precipitation associated with the front, while the SURF2 experiment (Fig. 7d) gives precipitation amounts closer than the observed ones (Fig. 7a). All the experiments overestimate precipitation over South-western France. On the French Riviera, the CTRL experiment underestimates the surface rainfall while the SAT_RAD_SURF2 and the SURF2 experiments overestimate it.

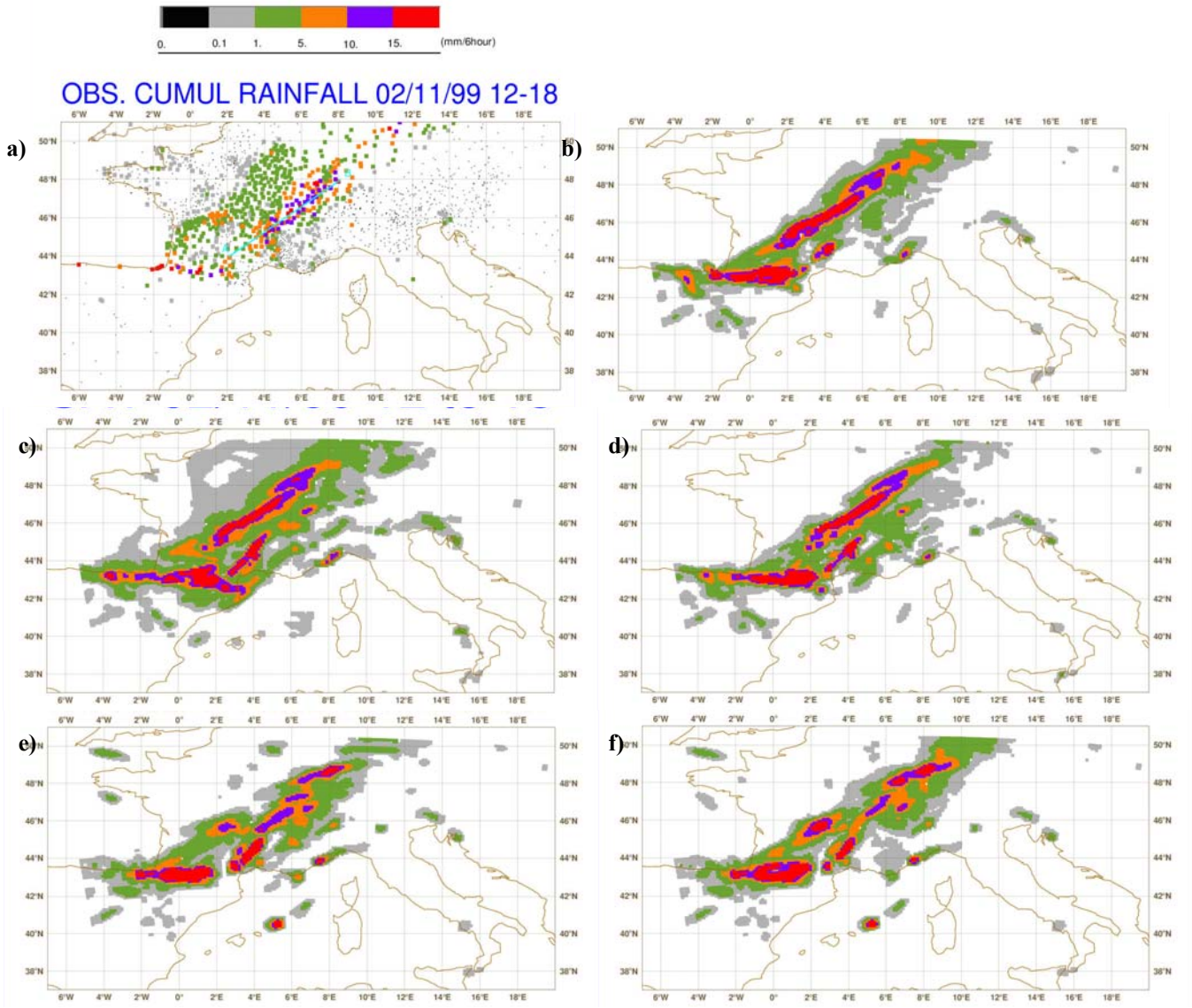

Figure 5 : *6-hour cumulated surface rainfall (mm) between 12 UTC, 2 Nov. 1999 and 18 UTC, 3 Nov. 1999 for the observations (a), the CTRL1 experiment (b), the SAT1 experiment (c), the SAT_RAD1 experiment (d), the SAT_RAD_SURF1 experiment (e), the SURF experiment (f).*

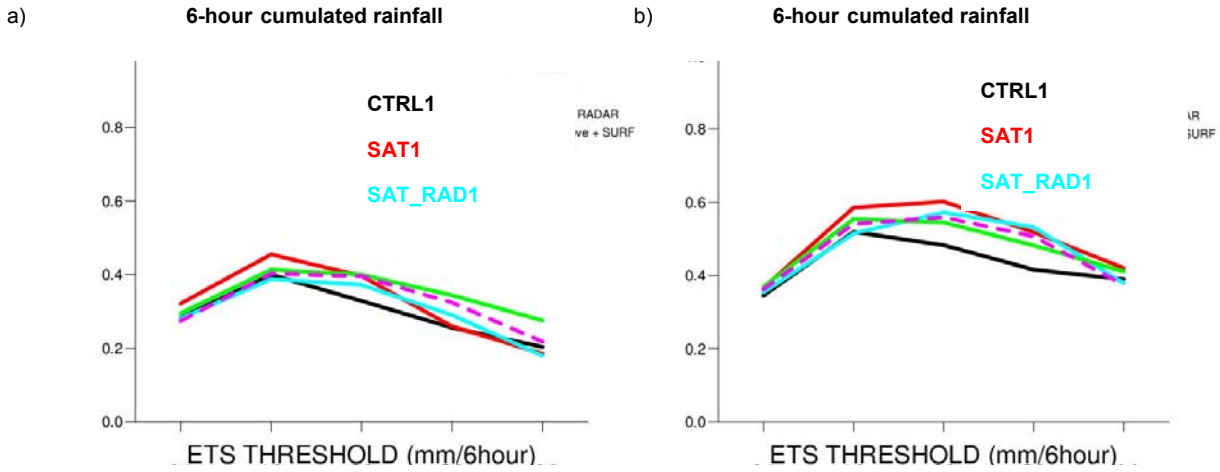

Figure 6 : *ETS scores for the CTRL1, SAT1, SAT_RAD1, SAT_RAD_SURF1 and the SURF1 experiments computed : a) on 6-hour cumulated rainfall for the first 24 hours of the simulation (12UTC, 2Nov. 1999 to 12UTC, 3 Nov. 1999) and on the 6-hour cumulated rainfall between 18UTC, 2 Nov. 1999 and 00 UTC, 3 Nov. 1999. Simulated and observed data have been averaged on circles of 30 km of radius centered on model grid points of the 10km domain.*

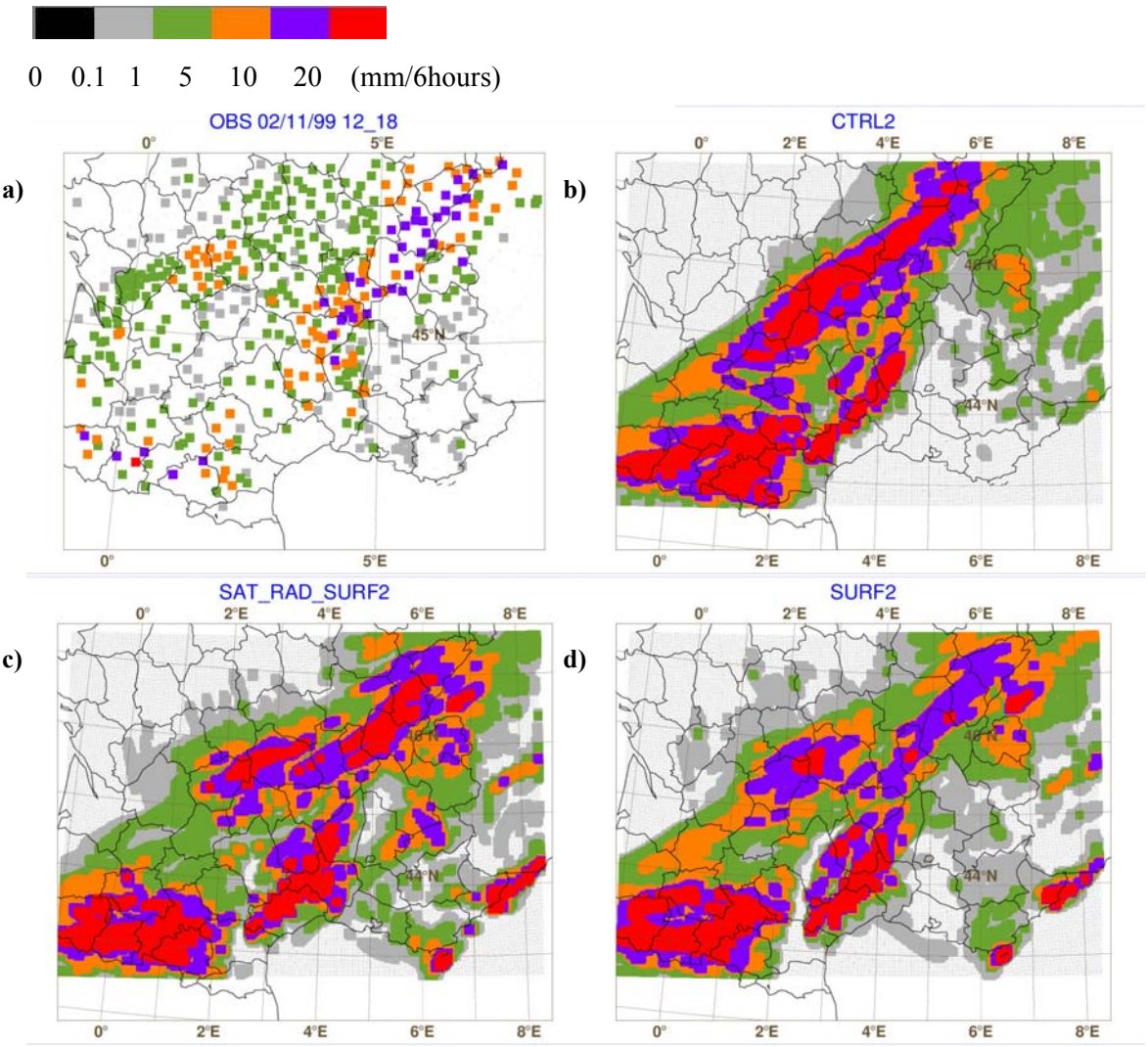

Figure 7 : *6-hour cumulated surface rainfall (mm) between 12 UTC, 2 Nov. 1999 and 18 UTC, 3 Nov. 1999 for the observations (a), the CTRL2 experiment (b), the SAT_RAD_SURF2 experiment (b), the SURF experiment (d).*

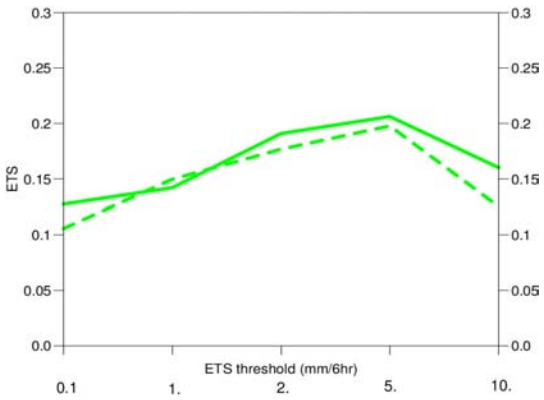

Figure 8 *: ETS for the SAT_RAD_SURF1(solid line) and SAT_RAD_SURF2 (dashed line) experiments computed on 6-hour cumulated rainfall for 12UTC, 2 Nov. 1999 to 18 UTC, 2Nov. 1999 and for different thresholds (0.1, 1.,2. ,5. and 10 mm). For each observations, the value of the nearest model grid-point has been compared on the 2.5 km domain.*

6. Summary and perspective

The results of the numerical experiments with two different methods to modify the initial conditions show that by modifying the initial state to take into account of moist areas identified by cloud classification or by radar reflectivity, one can obtain slight to significant improvements of the surface rainfall forecast. Both numerical experiments described in parts 4 and 5 stress the importance of the mesonet surface observations.

In the studies presented here, the synthetic humidity profiles produced by the pre-processing of cloud and precipitation data are analysed with OI scheme to update the initial state at 10 and 30 km resolutions or used directly to adjust the initial state at 2.5 km resolution. In a near future, it is planned to analyse these synthetic profiles with the 3D-Var Aladin/MESO-NH hybrid system. In this system, the analysis will be performed with the 3D-Var ALADIN analysis and the forward model will be MESO-NH with a 2.5 km resolution. Preliminary results based on the 3D-Var analysis/10 km Aladin model show encouraging results. It is also planned to use the Water Vapour channel of METEOSAT to estimate the relative humidity in clear air conditions instead of the present empirical values.

7. References

Bechtold, P. , E. Bazile, F. Guichard, P. Mascart and E. Richard, 2001: A mass flux convection scheme for regional and global models, Q. J. Roy. Meteor. Soc., 127, 869-886.

Bougeault P., P. binder, A. Buzzi, R. Dirks, R. Houze, J. Kuetner, R.B. Smith, R. Steinacker and H. Volkert, 2001: The map special observing period, Bull. Amer. Meteorol. Soc., 82, 3, 433-462.

Calas, C., V. Ducrocq and S. Sénési, 2000: Mesoscale analyses and dignostic parameters for deep convection nowcasting, Met. Applications , 7, 143-161.

Caniaux, G., J.-L. Redelsperger and J.-P. Lafore, 1994: A numerical study of the stratiform region of a fast-moving squall line. Part I. General description, and water and heat budgets. J. Atmos. Sci., 51, 2046-2074.

Clark, T.L., and R.D. Farley, 1984: Severe downslope windstorm calculations in two and three spatial dimensions using anelastic interactive grid nesting: A possible mechanism for gustiness. J. Atmos. Sci., 41, 329-350.

Desbois, M. G. Seze, and G. Szejwach, 1982: Automatic classification of clouds on METEOSAT imagery: application to high level clouds, J. Appl. Meteor., 21, 401-412.

Ducrocq, V., J.P. Lafore, J.L. Redelsperger and F. Orain, 2000 Initialisation of a fine scale model for convective system prediction: A case study, Q. J. Roy. Meteor. Soc., 126, 3041-3066.

Ducrocq, V., D. Ricard, J.P.Lafore and F. Orain, 2002: Storm-scale numerical rainfall prediction for five precipitating events over France: on the importance of the initial humidity field, accepted to Wea. Forecasting.

Gal-Chen,T. and R.C.J. Sommerville, 1975:On the use of a coordinate transformation for the solution of the Navier-Stokes equations, J. Comput.Phys., 17, 209-228.

Kain, J.S. and J.M. Fritsch, 1993: Convective parameterization for mesoscale models: the Kain-Fritsch scheme. The representation of cumulus convection in numerical models. Meteor. Monogr., N°24, Amer. Meteor. Soc. 165-170.

Lafore J.P., J. Stein, N. Asencio, P. Bougeault, V. Ducrocq, J. Duron, C. Fisher, P. Hereil, P. Mascart , V. Masson, J.P. Pinty, J.L. Redelsperger, E. Richard, J. Vila-Guerau de Arellano, 1998: The Meso-NH Atmospheric simulation system. Part I: adiabatic formulation and control simulations, Ann. Geophysicae, 16, 90-109

Stein, J., E. Richard, J.P. Lafore, J.P. Pinty, N. Asencio and S. Cosma, 2000: High-Resolution Non-Hydrostatic Simulations of Flash-Flood Episodes with grid-nesting and ice-phase parameterization, Meteor. Atmos. Physics,72, 203-221.